MicroRNA-27a-3p Relives Inflammation and Neurologic Impairment after Cerebral Ischemia Reperfusion via Inhibiting LITAF and the TLR4/NF-κB Pathway

Jing Luo
First Affilated Hospital of Kunming Medical University
Junjie Li
First Affiliated Hospital of Kunming Medical University
Li Xiong
First Affiliated Hospital of Kunming Medical University
Linna Fan
First People's Hospital of Yuxi
Lijia Peng
First Affiliated Hospital of Kunming Medical University
Yuan Yang
Second Affiliated Hospital of Kunming Medical University
Di Lu
Kunming Medical University
Jianlin Shao (cmushaojl@aliyun.com)
First Affiliated Hospital of Kunming Medical University

Research

Keywords: Cerebral ischemia reperfusion, Biliverdin, MicroRNA assay, Litaf, TLR4, NF-κB

Posted Date: October 23rd, 2020

DOI: https://doi.org/10.21203/rs.3.rs-93820/v1

Abstract

Background: Cerebral ischemia reperfusion (CIR) affects microRNA (miR) expression and causes substantial inflammation. Here, we investigated the influence and underlying mechanism of miR-27-3p in rats with CIR.

Methods: Cerebral ischemia reperfusion was built by tMCAO. Rats were randomly divided into Sham group, brain ischemic reperfusion (IR) group, brain ischemic reperfusion transfected with NC group, brain ischemic reperfusion transfected with miR-27a-3p mimic group, brain ischemic reperfusion transfected with miR-27a-3p inhibitor group and brain ischemic reperfusion transfected with miR-27a-3p mimic and Litaf mimic group. The relationship between miR-27a-3p and Litaf was verified via qRT-PCR and luciferase assays. The cellular distribution of Litaf was determined via double immunofluorescence. The effect of miR-27a-3p on the expression of Litaf, TLR4, NF-κB and IL-6 was evaluated using synthetic miR-27a-3p mimic and inhibitor. The level of Nissl's body in each group was detected by Nissl's staining. The infarct in each group was evaluated by TTC staining.

Results: Firstly, BV treatment relieves cerebral infarction and decreases the levels of serum IL-1β, IL-6 and TNF-α. Through our previous study, we found key microRNA mR-27a-3p and its targeted gene Litaf might involve in the molecular mechanism of CIR. Then, the regulation between miR-27a-3p and Litaf was verified by the temporal miR-27a-3p and Litaf expression profiles and luciferase assay. Moreover, intracerebroventricular injection of the miR-27a-3p mimic significantly decreased the Litaf, TLR4, NF-κB and interleukin (IL)-6 levels and the double-labeled cell count 24 h post-surgery, whereas miR-27a-3p inhibitor reversed these effects. Furthermore, miR-27a-3p mimic could relive cerebral infarct and neurologic deficit after CIR. In addition, injection of miR-27a-3p mimic decreased neuronal damage induced by CIR.

Conclusions: Increasing miR-27-3p levels protect against CIR by relieving inflammation, neuronal damage and neurologic deficit by inhibiting LITAF and the TLR4/NF-κB pathway.

Background

Stroke is one of the top ten causes of death in the world [1]. Brain ischemic stroke, one of the most destructive types of stoke, is a leading cause of death and severe disability in adults worldwide [2–4] and becoming a prominent public health risk [5, 6]. Generally, vascular recanalization to obtain timely reperfusion is the preferred treatment in clinical practice. However, reperfusion can induce further unexpected brain injury, termed cerebral ischemia reperfusion injury (CIR) [7]. Inflammatory is an important factor during ischemic stroke [8, 9]. Thus, anti-inflammatory therapy may lessen neurological deficits by ischemic stroke and it may serve as a potential therapeutic strategy following ischemic stroke [6].

Biliverdin (BV), a metabolite of heme catabolism, shows a protective role in lung graft injury, hemorrhagic shock and resuscitation-induced lung injury via anti-inflammatory and antioxidant mechanisms [10–12].

Previous study indicated that exogenously administered carbonic oxide (CO) and BV have potent cytoprotective role on intestinal ischemia reperfusion injury [13]. Moreover, BV treatment can relieve CIR in rats, and the mechanism may be associated with the downregulation of proinflammatory factors [12]. While previous studies have focused on the anti-inflammatory mechanism of BV, the molecular network upstream and downstream of BV remains unclear.

MicroRNAs (miRNAs) are a group of single-stranded non-coding RNAs with 20 ~ 22 nt in length and widely expressed in eukaryotes [14, 15]. MiRNAs have been suggested to exert their function by binding to the 3'UTRs of their target mRNAs at post-transcriptional level [16]. Studies have shown that several miRNAs can dramatically alter normal physiological processes and are involved in the pathogenesis of human diseases [17]. Accumulating evidence has demonstrated that aberrant expression of miRNAs play critical roles in central nervous system injury [18–20]. Among the miRNAs, miR-27-3p has been widely studies due to its important role in regulating inflammation and innate immune pathway [21–24]. However, little is known about the function of miR-27-3p in the interaction with lipopolysaccharide induced TNF factor (LITAF) in rat with CIR. Here, through our previous study, we found that BV treatment induced the upregulation of miR-27a-3p in cortex tissues in rats with cerebral ischemia reperfusion. Functional studies showed that improves neuron injury and neurologic impairment after cerebral ischemia reperfusion by inhibiting LITAF and the TLR4/NF-κB pathway.

Materials And Methods

Animals and groups

The Sprague-Dawley (SD) rats used in the study were purchased from the Laboratory Animal Research Center of Kunming Medical University. All experiments were approved by the Ethics Committee of Kunming Medical University. The SD rats were given free access to food and water and were housed at room temperature (22±2℃) with 45-50% humidity and a 12h light/dark cycle. Experiment 1: rats were randomly divided into Sham group, brain ischemic reperfusion (IR) group and brain ischemic reperfusion with BV treatment (BV) group. Experiment 2: rats were randomly divided into Sham group, brain ischemic reperfusion (IR) group, brain ischemic reperfusion transfected with NC (NC) group, brain ischemic reperfusion transfected with miR-27a-3p mimic (IR+miR-27a mimic) group, brain ischemic reperfusion transfected with miR-27a-3p inhibitor (IR+miR-27a inhibitor) group and brain ischemic reperfusion transfected with miR-27a-3p mimic and Litaf mimic (IR+miR-27a mimic+Litaf mimic) group.

Transient middle cerebral artery occlusion model and BV treatment

The right middle cerebral artery was occluded according to the standard operation procedures for transient middle cerebral artery occlusion (tMCAO) rat model [25, 26]. Briefly, animals were anaesthetized with 5 mg/kg xylazine HCl and 40 mg/kg ketamine HCl by an intraperitoneal (ip) injection. The right

common carotid artery (RCCA), right externalcarotid artery, and right internal carotid artery were isolated for inserting the nylon monofilament (diameter 0.24 mm; Johnson & Johnson, New Brunswick, NJ, USA). The monofilament was fixed in position tightly and then the incision was sutured. Rat body temperature was maintained at 36.5±0.5˚C using a heating lamp. A laser Doppler system (Peri-Flux System 5000; Perimed, Jarfalla, Sweden) was used to supervise regional cerebral blood flow (rCBF). Rats in the Sham group underwent the same procedures without inserting a nylon thread. After 2 h of tMCAO, CBF was recovered by removing the nylon thread, and the incision was closed. BV was diluted in saline and injected (35 mg/kg ip) to rats 15 min prior to reperfusion, then once again 4 h after reperfusion, and twice per day thereafter [12, 27]. In the Sham and IR groups, the same volume of saline was injected in the same way.

Intracerebroventricular injection of a synthetic miR-27-3p

Rats were intracerebroventricularly injected with virus vector (NC), miR-27a-3p mimic, miR-27a-3p inhibitor, miR-27a-3p mimic and LITAF mimic 7 days prior to CIR. The processes of injections were performed as previously described [28]. According to the manufacturer's guidelines, we intracerebroventricularly infused 15 μL of a synthetic miR-27-3p mimic, miR-27-3p inhibitor and a control mimic to regulate in vivo miR-27a-3p expression. After anesthetization with 5 mg/kg xylazine HCl and 40 mg/kg ketamine HCl, a stainless-steel microinjector was stereotaxically put into the left lateral ventricle at 0.6 mm posterior to bregma, 1.3 mm lateral from middle and 5.0 mm vertically from the skull surface. Intracerebroventricular injection were repeatedly performed for 3 days prior to ischemia.

Assessment of infarction volume

After 2h ischemia and 24h reperfusion, the animals were sacrificed, and the brains were coronally sectioned into 2-mm-thick in a rat brain matrix and stained in 2% 2,3,5-triphenyltetrazolium chloride (TTC) solution before fixation in 10% formalin overnight. The infarction area was imaged with a scanner and analyzed using Image J 1.4 (National Institute of Health, Bethesda, MD, USA). Infarct size was calculated and expressed as a percentage by using the following formula to eliminate effects of edema as described previously [29]: [(contralateral volume)−(ipsilateral undamaged volume)]×100/(contralateral volume).

Enzyme-linked immunosorbent assay (ELISA)

Both IL-1β, IL-6 and TNF-α in peripheral blood of rats in Sham, IR and BV groups were detected by ELISA. Refer to the kit instructions for specific detection steps.

Luciferase assay

Luciferase reporter assay was performed for investigating the relationship between miR-27a-3p and LITADF. Briefly, cells were co-transfected with 100ng LITAF 3'UTR wild type (WT) or LITAF 3'UTR-Mutant (Mut) plasmid, 5ng Renilla, and 2 μg mimics NC or miR-27a-3p expression plasmid all combined with LipofectamineTM 2000 reagent (supplied by Ribobio, Guangzhou, China). After cells were cultured for 24h at 37℃ with 5% CO_2, they were washed and lysed according to the manufacturer's protocol (Ribobio, Guangzhou, China). Finally, fluorescence value was detected using fluorescence light meter.

NSS score

Rats from the three groups were scored by an evaluator with modified neurological severity scores (NSS), as previously reported [30], at day 6h, 12h, 24h and 48h post-reperfusion. The NSS includes four physiological function evaluation scores: Feeling, movement, reflection and balance. Score 1-4 indicates mild injury, 4-8, moderate injury, and 8-12, severe injury. The neural behavioral test was conducted by an evaluator that was blinded to the treatments.

Water content of brain tissues

After 24 h of reperfusion, animals in Sham, NC group, IR group, IR+miR-27 mimic group, IR+ miR-27a-3p inhibitor group and IR+ miR-27a mimic+Litaf mimic group were anesthetized. Brains were extracted and weighed. Subsequently, tissue was dried at 105 °C for 24 h, and the dry weight documented. The % of brain water content was calculated using the following equation.

Double immunofluorescence analysis

Double immunofluorescence analysis was performed to detect LITAF and a neuronal marker (NeuN) and a microglial marker (Iba1) as previously described [2]. Briefly, 5 μm-thick sections were incubated overnight at 4℃ with the primary rabbit anti-LITAF (1:100, Abcam) and rat anti-NeuN (1:100, Abcam), rat anti-Iba1 (1:100, Abcam) antibodies. Then, the sections were incubated with Alexa 488-conjugated goat anti-rabbit IgG (1:500) and Alexa 594-conjugated goat anti-rat IgG (Molecular Probes, MA, USA) for 2 h at room temperature. Additionally, the interaction between LITAF and TLR4/NF-κB/IL-6 was explored using primary rabbit anti-LITAF and rat anti- TLR4/NF-κB/IL-6 antibodies as described above. Images were captured using a Leica confocal microscope (Leica Microsystems, Buffalo Grove, IL, USA).

Nissl staining and neuron count

Rats were subjected to deep anesthesia after neurological deficit examination. After perfusion, the brain was fixed for 48h, dehydrated, and embedded in wax. Coronal slices at 25μm thick were set for Nissl staining and immunofluorescence staining trials. The experiment was performed in accordance with the instruction of Nissl staining kit (Solarbio, China). After dehydrated with alcohol and then immersed in

xylene, brain slices were stained with thionine. Then, cell morphological alteration of cortex was observed by microscopy. Number of surviving neurons in the cortex was recorded via neurons count.

Real-time fluorescence quantitative PCR

After total RNA was extracted from cortex in different groups using the Trizol reagent (Invitrogen), total RNA was reversely transcribed into cDNA using RT reagent Kit (TAKATA, Japan). Then, q-PCR analysis was performed to quantify the expression level of miR-27a-3p and LITAF using an SYBR Green RT-PCR Master Mix kit (TAKARA, Japan), respectively. The primers were shown as follow. Then the reaction was performed at 95℃ for 2min; and circulated 40 times at 95℃ for 15s, 60℃ for 30s and 60℃ for 40s. The fluorescence were collected and recorded after finishing 40 cycles. All reaction was processed on real time fluorescent quantitative PCR (ABI 7500). The cycle number (Ct) was obtained for each independent amplification reaction. The relative gene expression levels were calculated using the comparative Ct (△△Ct) method, where the relative expression is calculated as $2^{-\triangle\triangle Ct}$.

Western blot

Cortex from different groups were plated in 60-mm tissue culture plates. After the tissues were washed twice with cold PBS, total protein were extracted by adding 100μl lysis buffer (BD Biosciences, San Jose, CA) with protease inhibitor cocktail (Calbiochem, La Jolla, CA). Then, after the proteins were separated on a SDS-PAGE gel for 2h at 350mA, they were transferred to PVDF membranes for 2h at 350mA. After the transfer was completed, the PVDF membranes were washed with 1×TBST, and then placed in 5% BSA and slowly swayed for 2h. Then, the PVDF membranes were incubated with different primary antibodies Litaf (Abcam, 1:2000), TLR4 (1:1000), p-p65(1:1000), p-65(1:1000), IL-6 (1:500) and β-actin (1:1000) overnight at 4℃, respectively. Afterwards, the PDVF membranes were incubated with the secondary antibody (1:2000) for 2h at room temperature after they were rapidly washed three times with 1×TBST for 5min. Finally, after the PVDF membranes were washed three times with 1×TBST for 5min, they were scanned in Alpha Innotech (BioRad) with ECL.

Statistical analysis

All data were expressed as the mean ± standard deviation (SD). Statistical comparisons were performed between two groups using t-test and among multiple groups by ANOVA. A value of $P < 0.05$ was considered to be statistically significant.

Results

BV treatment relieves cerebral infarction and decreases the levels of serum IL-1β, IL-6 and TNF-α

TTC staining was used to detect the cerebral infarction volume at 24h after reperfusion to verify whether BV administration could improve functional deficits in rats with CIR. We found that the infarct volume percentage (%) in IR group was significantly larger than that in Sham group (P<0.05, Fig. 1A and 1B). The infarct volume percentage (%) in BV group was obviously reduced than that in IR group (P<0.05, Fig. 1B), suggesting that BV could relieve cerebral infarct caused by cerebral ischemia reperfusion injury. According to the results of ELISA, the rats in IR group had a higher levels of IL-1β, IL-6 and TNF-α in the serum than those in the Sham group, while the levels of IL-1β, IL-6 and TNF-α in the serum in BV group were evidently decreased compared with those in IR group (P<0.05, Fig. 1C).

BV treatment induced abnormal microRNAs expression

We used microRNA microarray analysis to detect the expression profiles of miRNAs in cortex tissues isolated from rats in Sham, IR and BV groups in our previous study. According to the results of miRNA microarray, we selected the top 10 differentially expressed miRNAs to perform for heatmap (Fig. 2A). miRWalk, miRDB and TargetScan databases were used to predict the targeted genes of miR-27a-3p. There are 838, 667, 990 targeted genes of miR-27a-3p from miRWalk, miRDB and TargetScan databases (Fig. 2B), among them, 42 genes are common. Then, Cytoscape was used to draw interaction network between miR-27a-3p and its common targeted genes (Fig. 2C).

GO and KEGG pathway analysis of targeted genes of miR-27a-3p

To explicit the biological function of miR-27a-3p, we performed for GO analysis of 42 targeted genes of miR-27a-3p. We found that the top 10 biological processes (BP) of 42 targeted genes of miR-27a-3p were cellular macromolecule metabolic process, cellular protein modification process, cellular response to stress, macromolecule modification, positive regulation of biological process, positive regulation of cellular process, protein modification process, regulation of nucleobase containing compound metabolic, regulation of striated muscle tissue development and response to stress. The top 10 cellular component (CC) were intracellular membrane bounded organelle, intracellular organelle, intracellular organelle lumen, membrane bounded organelle, membrane enclosed lumen, nuclear lumen, nuclear part, nucleus, organelle and organelle lumen. The top 10 molecular function (MF) were kinase activity, phosphotransferase activity, protein binding, protein kinase activity, receptor activator activity, receptor agonist activity, receptor regulator activity, transcription factor activity, transcription factor activity and protein binding and transferase activity (Fig. 3A).

To reveal the pathways of miR-27a-3p, we performed for KEGG pathway analysis of 42 targeted genes of miR-27a-3p. Results showed that the top 5 pathways of 42 targeted genes of miR-27a-3p were p53 signaling pathway, Wnt signaling pathway, mTOR signaling pathway, cGMP-PKG signaling pathway and

regulation of autophagy (Fig. 3B). Among them, the targeted gene LITAF of miR-27a-3p mainly involved in p53 signaling pathway and regulation of autophagy.

LITAF as a target of miR-27a-3p

The target sites of miR-27a-3p in the 3'UTR of LITAF were shown in Fig. 4A. In order to experimentally confirm information, portions of the 3'UTR of these potential targets were cloned into pGL3 control vector, downstream of luciferase-coding sequences. The recombinational plasmids of 3'UTR of LITAF-WT or 3'UTR of LITAF-MUT were co-transfected with miR-27a-3p or miR-27a-3p (mimic NC) and Renilla into cells. The relative luciferase activity was decreased in cells co-transfected with miR-27a-3p and 3'UTR of LITAF compared with cells co-transfected with mimic NC and 3'UTR of LITAF, there is no significant difference in relative luciferase activity between cells co-transfected with mimic NC and 3'UTR of LITAF-MUT compared with cells co-transfected with miR-27a-3p and 3'UTR of LITAF-MUT (Fig. 4B). These results suggested that miR-27a-3p can negatively regulate LITAF.

Temporal expression of miR-27-3p and LITAF after CIR

The CIR-induced changes in the miR-27-3p and LITAF expression levels were examined for 24 h post-surgery. MiR-27-3p expression was obviously downregulated with time and reached its lowest levels at both 24 and 48 h after CIR compared with the levels in the Sham group (Fig. 5A, $P < 0.05$). Likewise, the LITAF expression levels were significantly increased beginning from 6 h after IR, and this high level reached its highest levels at 24 and 48h after CIR maintained throughout the observation period (Fig. 5B, $P < 0.05$), suggesting a potential negative correlation between miR-27-3p and LITAF expression (Fig.5C).

Expression levels of miR-27a-3p and LITAF in cortex of rat transfected with lentivirus

Seven day after transfected lentiviru, qRT-PCR was used to detect relative expression levels of miR-27a-3p and Litaf in rats. We found that relative expression level of miR-27a-3p was increased in miR-27a-3p mimic group ($P<0.01$, Fig. 6A), while decreased in miR-27a-3p inhibitor group ($P<0.05$, Fig. 6A). Moreover, to investigate the effect of overexpression of Litaf on miR-27a-3p, we injected Litaf mimic at the same. We found that relative expression of Litaf was increased in Litaf mimic group (Fig. 6B).

MicroRNA-27a-3p relives neurologic deficit after cerebral ischemia reperfusion

To determine the effect of miR-27-3p on the neurological function in rats with CIR, NSS was used to assess the functional recovery. The NSS test was performed at 6h, 12h, 24h and 48h post-reperfusion in

Sham, IR, IR+NC, IR+miR-27a-3p mimic, IR+miR-27a-3p inhibitor and IR+miR-27a-3p mimic + Litaf mimic groups. We found that NSS score showed similar tendency in six groups at four sampling time (Fig. 7A). We focus the NSS scores in six groups at 24h post-reperfusion. Compared with the Sham group, functional deficits were impaired by ischemic insult in the IR group at 6h, 12h, 24h and 48h post-reperfusion ($P<0.01$; Fig. 7B). A slight recovery of neurological functions was observed in the IR+miR-27a-3p mimic group, while a slight exacerbation of neurological functions was found in the IR+miR-27a-3p inhibitor and IR+miR-27a-3p mimic + Litaf mimic groups at 6h, 12h, 24h and 48h post-reperfusion (Fig. 7B). Therefore, it can be concluded that miR-27a-3p mimic effectively decreased cerebral infarction volume and may improve functional recovery.

MiR-27a-3p mimic relieves cerebral infarct induced by CIR

TTC staining was used to detect the cerebral infarction volume at 24h after reperfusion to verify whether miR-27a-3p mimic administration could improve functional deficits in rats with CIR. We found that the infarct volume percentage (%) in IR group was significantly larger than that in Sham group ($P<0.05$, Fig. 8A and 8B). The infarct volume percentage (%) in IR+miR-27a-3p mimic group was obviously reduced than that in IR group ($P<0.05$, Fig. 8B), while in IR+miR-27a-3p inhibitor was increased than that in IR group, suggesting that miR-27a-3p overexpression could relieve cerebral infarct caused by cerebral ischemia reperfusion injury.

MiR-27a-3p mimic inhibits the fluorescence signal for LITAF in neuron and microglial cell

As shown in Fig. 9A and 9B, the majority of the fluorescence signal for LITAF in the IR group was localized in the cells positive for NeuN and Iba1 (cells with yellow signals) at both 24 h after IR. Representative photomicrographs and quantification showed that miR-27a-3p mimic injection significantly decreased LITAF immunoreactivity and the number of LITAF-positive double-labeled cells in the neurons and microglia (Fig. 9A, 9B and 9C, $P<0.05$), while increased LITAF immunoreactivity and the number of LITAF-positive double-labeled cells was observed with miR-27a-3p inhibitor injection, no such change was observed with miR-27a-3p control injection (IR+NC group). These effects in response to miR-27a-3p mimic were also increased by the addition of LITAF mimic (Fig. 9A, B, C, $P < 0.05$). No significant differences were found between the IR and IR+NC groups ($P > 0.05$).

MiR-27a-3p mimic deceases neuronal damage induced by CIR

After 24h of reperfusion, Nissl staining was employed to exhibit morphological alterations in cortex. Normal neurons were polygonal and the nissl bodies were blue patches in the cytoplasm in Sham group

(Fig. 10A), while nissl bodies were dissolved in IR group (Fig. 10A). However, in IR+miR-27a-3p mimic group, these changes were rare (Fig. 10A). Neurons count in cortex examined the quantity of positive stained neurons (Fig. 10B). Compared with Sham group, surviving neurons count of IR declined significantly. Surviving neurons were increased obviously after injection of miR-27a-3p mimic, while decreased obviously after injection of miR-27a-3p inhibitor (Fig.10B).

MiR-27a-3p modulate Litaf to release IL-6

Double immunofluorescence analysis was used to verify whether miR-27a-3p could regulate Litaf to release IL-6. We found that Litaf/IL-6 were both co-expressed at 24h after reperfusion in cortex of rats (Fig. 11A). Litaf/IL-6 double positive cells were increased in IR and IR+NC groups compared with those in Sham group (P<0.05) (Fig. 12B and C). After addition of miR-27a-3p mimic, Litaf/IL-6 double positive cells were decreased than those in IR and IR+NC group (P<0.05, Fig. 12B and C). Litaf/IL-6 double positive cells in IR+miR-27a-3p mimic+Litaf mimic groups were increased compared with those in IR+miR-27a-3p group (Fig. 11B and C). Western blot was used to detect the effect of miR-27a-3p on the protein expression of IL-6. We found that the relative protein expression levels of IL-6 were increased in IR and IR+NC groups compared with these in Sham group (P<0.05, Fig. 11D-E). While, after injection of miR-27a-3p mimic, relative protein expression levels of IL-6 were decreased in IR+miR-27a-3p compared with these IR and IR+NC group (P<0.05, Fig. 11D-E). ELISA results showed that serum IL-6 level was increased in IR and IR+NC group than that in Sham group (P<0.05, Fig. 12F). After addition of miR-27a-3p inhibitor, serum IL-6 level was increased than that in IR and IR+NC group (P<0.05, Fig. 11F), the same result was seen in IR+miR-27a-3p mimic+Litaf mimic group (P<0.05, Fig. 11F).

MiR-27a-3p regulates Litaf through TLR4/NF-κB

Double immunofluorescence analysis was used to verify whether miR-27a-3p could regulate Litaf though TLR4/NF-κB signal pathway. We found that Litaf/TLR4, Litaf/ NF-κB were both co-expressed (Fig. 12A-B). Western blot was used to detect the effect of miR-27a-3p on the protein expression of Litaf, TLR4, NF-κB, p-p65 and p65. We found that the relative protein expression levels of Litaf, TLR4 and p-p65 were increased in IR and IR+NC groups compared with these in Sham group (P<0.05, Fig. 12C-D). While, after injection of miR-27a-3p mimic, relative protein expression levels of Litaf, TLR4 and p-p65 were decreased in IR+miR-27a-3p compared with these IR and IR+NC group (P<0.05, Fig. 12C-D).

Discussion

CIR injury, one of the major causes of death from stoke in the world, not only causes tremendous damage to human health, but also brings heavy economic burden to family and society [31, 32]. CIR injury is a complex pathological process, and a study found that neuronal injury in the brain is an important cause

of reperfusion injury [33, 34]. Therefore, how to protect brain neuronal cells from CIR injury is an important research.

Here, firstly, we injected BV into rats prior to reperfusion. We found that BV could relieve cerebral infarct caused by CIR injury at 24h post-reperfusion. Previous study indicated BV administration decreased cerebral infarction volume at 48h post-reperfusion [12, 27]. Meanwhile, BV administration could decrease the levels of serum IL-1β, IL-6 and TNF-α compared with these in IR group. Previous study demonstrated that BV could decrease the expression of IL-1β, IL-6 and TNF-α at mRNA and protein levels [27]. Our results further confirmed previous studies.

Numerous studies have indicated that expressions of miRNAs would be changed in the brain in response to CIR [35-37]. Thus, elucidation of specific miRNA is regarded as a potential target against CIR injury. In the study, we found a key miR-27a-3p and its targeted Litaf might participate in the molecular mechanism of CIR. MiR-27a-3p has been identified to be implicated in several types of human malignancies, including thyroid cancer [38], breast cancer [39], gastric cancer [40] and esophageal cancer [41]. LITAF is a mediator of local and systemic inflammatory responses [42] and is locally upregulated in many inflammatory diseases, such as Crohn disease and ulcerative colitis [43]. Our study firstly confirmed the regulation between miR-27a-3p and Litaf by the luciferase assay, temporal miR-27a-3p and Litaf expression profiles in rats with CIR injury.

Our results indicated that miR-27a-3p mimic could relive cerebral infarct and neurologic deficit after CIR, while miR-27a-3p inhibitor led to the opposite results. Previous study indicated that intracerebroventricular injection of miR-494 agomir reduced cerebral infarct volume at the acute stage of MCAO [44]. MiR-421 antagomir significantly decreased infarction volumes in rats with CIR injury[45]. Inhibition of miR-30a, even at 90 min post onset of middle cerebral artery occlusion, reduced infarct volume [46]. MiR-199a-5p improved neurological deficit of rats with CIR injury [47]. MiR-181a inhibition neurologic defict in female mice subjected to middle cerebral artery occlusion [48]. These results suggested that miRNAs involved in improving the injury caused by CIR.

Intracerebroventricular injection of the miR-27a-3p mimic significantly decreased the mRNA expression of Litaf and IL-6, and serum IL-6 at 24 h post-surgery, whereas miR-27a-3p inhibitor reversed these effects. IL-6 is pleiotropic cytokine involved in many central nervous system disorders including stroke, and elevated serum IL-6 was found in acute stroke patients [49] and rats with CIR injury [50]. Intracerebroventricular injection of the miR-27a-3p mimic significantly decreased the TLR4 and NF-κB levels and the double-labeled cell count 24 h post-surgery, whereas miR-27a-3p inhibitor reversed these effects. Previous study indicated that ciprofloxacin and levofloxacin attenuate microglia inflammatory response by TLR4/NF-κB pathway [51]. Curcumin administration may improve neuroinflammatory outcomes by decreasing microglia/macrophage activation and neuronal apoptosis through TLR4/MyD88/NF-κB [52]. MiR-146a inhibited the inflammatory response of rheumatoid arthritis fibroblast-like synoviocytes by down-regulating TLR4/NF-κB pathway [53]. Our study is the first time to report that miR-27a-3p could attenuate inflammatory by inhibiting Litaf via TLR4/NF-κB pathway.

Conclusions

BV treatment relieves cerebral infarction and decreases the levels of serum IL-1β, IL-6 and TNF-α. Through bioinformatics prediction, we found that key mR-27a-3p and its targeted gene Litaf might involve in the molecular mechanism of CIR. Then, the regulation between miR-27a-3p and Litaf was verified by the temporal miR-27a-3p and Litaf expression profiles and luciferase assay. Moreover, intracerebroventricular injection of the miR-27a-3p mimic significantly decreased the Litaf, IL-6, TLR4 and NF-κB levels and the double-labeled cell count 24 h post-surgery, whereas miR-27a-3p inhibitor reversed these effects. Furthermore, miR-27a-3p mimic could relive cerebral infarct and neurologic deficit after CIR. In addition, injection of miR-27a-3p mimic decreased neuron injury induced by CIR. Increasing miR-27-3p levels protect against CIR by relieving inflammation, neuronal damage and neurologic deficit by inhibiting LITAF and the TLR4/NF-κB pathway (Fig. 13).

Abbreviations

BV: Biliverdin

CIR: Cerebral ischemia reperfusion

ELISA: Enzyme-linked immunosorbent assay

IR: Ischemic reperfusion

LITAF: lipopolysaccharide induced TNF factor

NF-κB: Nuclear factor kappa-B

miR: MicroRNA

Mut: Mutant

NSS: Neurological severity scores

SD: Sprague-Dawley

TLR4: Toll like receptor 4

tMCAO: Transient middle cerebral artery occlusion

TNF: Tumor necrosis factor

TTC: Triphenyltetrazolium chloride

WT: Wild type

Declarations

Availability of data and materials

Not applicable.

Acknowledgements

Not applicable.

Funding

This work was supported by the National Nature Science Foundation of China (81760248 and 81960250), Key Applied Basic Research program of Yunnan Province (2018FA042), Industry technology leading talent training program in Yunnan (YLXL20170054), Weifeng Yu Expert Workstation project (2017IC067) and Applied Basic Research Joint Project of Yunnan Province (2017FE468(-034)).

Author Contributions

JL and JLS designed the experiments and reviewed the paper. JL, JJL, and LX carried out the experiments. JL, LNF, LJP, YY and DL participated in the data acquisition and analysis. JL, DL and JLS wrote the manuscript and revised the manuscript. All authors read and approved the final manuscript.

Ethics declarations

Ethic approval and consent to participate

This study involves animal experiment and includes a statement on ethics approval.

Consent for publication

No applicable.

Competing interest

The authors declare that they have no conflict of interest.

References

1. Wang J, Cao B, Han D, Sun M, Feng J: Long non-coding RNA H19 induces cerebral ischemia reperfusion injury via activation of autophagy. *Aging Dis* 2017, 8:71-84.
2. Gao BY, Sun CC, Xia GH, Zhou ST, Zhang Y, Mao YR, Liu PL, Zheng Y, Zhao D, Li XT, et al: Paired associated magnetic stimulation promotes neural repair in the rat middle cerebral artery occlusion model of stroke. *Neural Regen Res* 2020, 15:2047-2056.
3. Sarrafzadegan N, Mohammmadifard N: Cardiovascular disease in Iran in the last 40 years: prevalence, mortality, morbidity, challenges and strategies for cardiovascular prevention. *Arch Iran Med* 2019, 22:204-210.
4. Mozaffarian D, Benjamin EJ, Go AS, Arnett DK, Blaha MJ, Cushman M, Das SR, de Ferranti S, Despres JP, Fullerton HJ, et al: Heart disease and stroke statistics-2016 update: a report from the American heart association. *Circulation* 2016, 133:e38-360.
5. Zhou XQ, Zeng XN, Kong H, Sun XL: Neuroprotective effects of berberine on stroke models in vitro and in vivo. *Neurosci Lett* 2008, 447:31-36.
6. Chen GY, Nunez G: Sterile inflammation: sensing and reacting to damage. *Nat Rev Immunol* 2010, 10:826-837.
7. Deng H, Zuo X, Zhang J, Liu X, Liu L, Xu Q, Wu Z, Ji A: Alphalipoic acid protects against cerebral ischemia/reperfusion-induced injury in rats. *Mol Med Rep* 2015, 11:3659-3665.
8. Lavine SD, Hofman FM, Zlokovic BV: Circulating antibody against tumor necrosis factor-alpha protects rat brain from reperfusion injury. *J Cereb Blood Flow Metab* 1998, 18:52-58.
9. Mo Y, Sun YY, Liu KY: Autophagy and inflammation in ischemic stroke. *Neural Regeneration Research* 2020, 15:1388-1396.
10. Fondevila C, Shen XD, Tsuchiyashi S, Yamashita K, Csizmadia E, Lassman C, Busuttil RW, Kupiec-Weglinski JW, Bach FH: Biliverdin therapy protects rat livers from ischemia and reperfusion injury. *Hepatology* 2004, 40:1333-1341.
11. Kosaka J, Morimatsu H, Takahashi T, Shimizu H, Kawanishi S, Omori E, Endo Y, Tamaki N, Morita M, Morita K: Effects of biliverdin administration on acute lung injury induced by hemorrhagic shock and resuscitation in rats. *PLoS One* 2013, 8:e63606.
12. Zou ZY, Liu J, Chang C, Li JJ, Luo J, Jin Y, Ma Z, Wang TH, Shao JL: Biliverdin administration regulates the microRNA-mRNA expressional network associated with neuroprotection in cerebral ischemia reperfusion injury in rats. *Int J Mol Med* 2019, 43:1356-1372.
13. Nakao A, Kaczorowski DJ, Sugimoto R, Billiar TR, McCurry KR: Application of heme oxygenase-1, carbon monoxide and biliverdin for the prevention of intestinal ischemia/reperfusion injury. *J Clin Biochem Nutr* 2008, 42:78-88.
14. Danbaran GR, Aslani S, Sharafkandi N, Hemmatzadeh M, Hosseinzadeh R, Azizi G, Jadidi-Niaragh F, Babaie F, Mohammadi H: How microRNAs affect the PD-L1 and its synthetic pathway in cancer. *Int Immunopharmacol* 2020, 84:106594.
15. Song Q, An Q, Niu B, Lu X: Role of miR-221/222 in tumor development and the underlying mechanism. *J Oncol* 2019, 2019:7252013.

16. Bartel DP: MicroRNAs: target recognition and regulatory functions. *Cell* 2009, 136:215-233.
17. Carthew RW, Sontheimer EJ: Origins and Mechanisms of miRNAs and siRNAs. *Cell* 2009, 136:642-655.
18. Bhalala OG, Srikanth M, Kessler JA: The emerging roles of microRNAs in CNS injuries. *Nat Rev Neurol* 2013, 9:328-339.
19. Guo D, Liu J, Wang W, Hao F, Sun X, Wu X, Bu P, Zhang Y, Liu Y, Liu F, et al: Alteration in abundance and compartmentalization of inflammation-related miRNAs in plasma after intracerebral hemorrhage. *Stroke* 2013, 44:1739-1742.
20. Wang SW, Liu Z, Shi ZS: Non-coding RNA in acute ischemic stroke: mechanisms, biomarkers and therapeutic targets. *Cell Transplant* 2018, 27:1763-1777.
21. Lv YN, Ou-Yang AJ, Fu LS: MicroRNA-27a Negatively Modulates the Inflammatory Response in Lipopolysaccharide-Stimulated Microglia by Targeting TLR4 and IRAK4. *Cell Mol Neurobiol* 2017, 37:195-210.
22. Cheng Y, Du L, Jiao H, Zhu H, Xu K, Guo S, Shi Q, Zhao T, Pang F, Jia X, Wang F: Mmu-miR-27a-5p-Dependent Upregulation of MCPIP1 Inhibits the Inflammatory Response in LPS-Induced RAW264.7 Macrophage Cells. *Biomed Res Int* 2015, 2015:607692.
23. Li XQ, Lv HW, Wang ZL, Tan WF, Fang B, Ma H: MiR-27a ameliorates inflammatory damage to the blood-spinal cord barrier after spinal cord ischemia: reperfusion injury in rats by downregulating TICAM-2 of the TLR4 signaling pathway. *J Neuroinflammation* 2015, 12:25.
24. Xie N, Cui H, Banerjee S, Tan Z, Salomao R, Fu M, Abraham E, Thannickal VJ, Liu G: miR-27a regulates inflammatory response of macrophages by targeting IL-10. *J Immunol* 2014, 193:327-334.
25. Chiang T, Messing RO, Chou WH: Mouse model of middle cerebral artery occlusion. *J Vis Exp* 2011.
26. Zhang Y, Shan Z, Zhao Y, Ai Y: Sevoflurane prevents miR-181a-induced cerebral ischemia/reperfusion injury. *Chem Biol Interact* 2019, 308:332-338.
27. Li JJ, Zou ZY, Liu J, Xiong LL, Jiang HY, Wang TH, Shao JL: Biliverdin administration ameliorates cerebral ischemia reperfusion injury in rats and is associated with proinflammatory factor downregulation. *Exp Ther Med* 2017, 14:671-679.
28. Shi QJ, Xiao L, Zhao B, Zhang XY, Wang XR, Xu DM, Yu SY, Fang SH, Lu YB, Zhang WP, et al: Intracerebroventricular injection of HAMI 3379, a selective cysteinyl leukotriene receptor 2 antagonist, protects against acute brain injury after focal cerebral ischemia in rats. *Brain Res* 2012, 1484:57-67.
29. Andrabi SS, Ali M, Tabassum H, Parveen S, Parvez S: Pramipexole prevents ischemic cell death via mitochondrial pathways in ischemic stroke. *Dis Model Mech* 2019, 12.
30. Eady TN, Khoutorova L, Obenaus A, Mohd-Yusof A, Bazan NG, Belayev L: Docosahexaenoic acid complexed to albumin provides neuroprotection after experimental stroke in aged rats. *Neurobiol Dis* 2014, 62:1-7.
31. Zuo G, Zhang D, Mu R, Shen H, Li X, Wang Z, Li H: Resolvin D2 protects against cerebral ischemia/reperfusion injury in rats. 2018, 11:9.

32. Long Y, Yang Q, Xiang Y, Zhang Y, Wan J, Liu S, Li N, Peng W: Nose to brain drug delivery - A promising strategy for active components from herbal medicine for treating cerebral ischemia reperfusion. *Pharmacol Res* 2020, 159:104795.
33. Yaidikar L, Byna B, Thakur SR: Neuroprotective effect of punicalagin against cerebral ischemia reperfusion-induced oxidative brain injury in rats. *J Stroke Cerebrovasc Dis* 2014, 23:2869-2878.
34. Liu W, Miao Y, Zhang L, Xu X, Luan Q: MiR-211 protects cerebral ischemia/reperfusion injury by inhibiting cell apoptosis. *Bioengineered* 2020, 11:189-200.
35. Fu C, Chen S, Cai N, Liu Z, Wang P, Zhao J: Potential neuroprotective effect of miR-451 against cerebral ischemia/reperfusion injury in stroke patients and a mouse model. *World Neurosurg* 2019, 130:e54-e61.
36. Sabirzhanov B, Matyas J, Coll-Miro M, Yu LL, Faden AI, Stoica BA, Wu J: Inhibition of microRNA-711 limits angiopoietin-1 and Akt changes, tissue damage, and motor dysfunction after contusive spinal cord injury in mice. *Cell Death Dis* 2019, 10:839.
37. Ghafouri-Fard S, Shoorei H, Taheri M: Non-coding RNAs participate in the ischemia-reperfusion injury. *Biomed Pharmacother* 2020, 129:110419.
38. Wang YL, Gong WG, Yuan QL: Effects of miR-27a upregulation on thyroid cancer cells migration, invasion, and angiogenesis. *Genet Mol Res* 2016, 15.
39. Tang W, Zhu J, Su S, Wu W, Liu Q, Su F, Yu F: MiR-27 as a prognostic marker for breast cancer progression and patient survival. *Plos One* 2012, 7.
40. Zhang Z, Liu S, Shi R, Zhao G: miR-27 promotes human gastric cancer cell metastasis by inducing epithelial-to-mesenchymal transition. *Cancer Genetics* 2011, 204:486-491.
41. Tanaka K, Miyata H, Sugimura K, Fukuda S, Kanemura T, Yamashita K, Miyazaki Y, Takahashi T, Kurokawa Y, Yamasaki M, et al: miR-27 is associated with chemoresistance in esophageal cancer through transformation of normal fibroblasts to cancer-associated fibroblasts. *Carcinogenesis* 2015, 36:894-903.
42. Merrill JC, You J, Constable C, Leeman SE, Amar S: Whole-body deletion of LPS-induced TNF-alpha factor (LITAF) markedly improves experimental endotoxic shock and inflammatory arthritis. *Proc Natl Acad Sci U S A* 2011, 108:21247-21252.
43. Huang Y, Bennett CL: Litaf/Simple protein is increased in intestinal tissues from patients with CD and UC, but is unlikely to function as a transcription factor. *Inflamm Bowel Dis* 2007, 13:120-121.
44. Zhao H, Li G, Zhang S, Li F, Wang R, Tao Z, Ma Q, Han Z, Yan F, Fan J, et al: Inhibition of histone deacetylase 3 by MiR-494 alleviates neuronal loss and improves neurological recovery in experimental stroke. 2019, 39:2392-2405.
45. Yue Y, Zhao H, Yue Y, Zhang Y, Wei W: Downregulation of microrna-421 relieves cerebral ischemia/reperfusion injuries: involvement of anti-apoptotic and antioxidant activities. *Neuromolecular Med* 2020.
46. Wang P, Pan R, Weaver J, Jia M, Yang X, Yang T, Liang J, Liu KJ: MicroRNA-30a regulates acute cerebral ischemia-induced blood-brain barrier damage through ZnT4/zinc pathway. *J Cereb Blood*

Flow Metab 2020:271678x20926787.

47. Li M, Luan L, Liu Q, Liu Y, Lan X, Li Z, Liu W: MiRNA-199a-5p protects against cerebral ischemic injury by down-regulating DDR1 in rats. *World Neurosurg* 2019, 131:e486-e494.
48. Stary CM, Xu L, Li L, Sun X, Ouyang YB, Xiong X, Zhao J, Giffard RG: Inhibition of miR-181a protects female mice from transient focal cerebral ischemia by targeting astrocyte estrogen receptor-α. *Mol Cell Neurosci* 2017, 82:118-125.
49. Suzuki S, Tanaka K, Suzuki N: Ambivalent aspects of interleukin-6 in cerebral ischemia: inflammatory versus neurotrophic aspects. *J Cereb Blood Flow Metab* 2009, 29:464-479.
50. Li TF, Ma J, Han XW, Jia YX, Yuan HF, Shui SF, Guo D, Yan L: Chrysin ameliorates cerebral ischemia/reperfusion (I/R) injury in rats by regulating the PI3K/Akt/mTOR pathway. *Neurochem Int* 2019, 129:104496.
51. Zusso M, Lunardi V, Franceschini D, Pagetta A, Lo R, Stifani S, Frigo AC, Giusti P, Moro S: Ciprofloxacin and levofloxacin attenuate microglia inflammatory response via TLR4/NF-kB pathway. *J Neuroinflammation* 2019, 16:148.
52. Zhu HT, Bian C, Yuan JC, Chu WH, Xiang X, Chen F, Wang CS, Feng H, Lin JK: Curcumin attenuates acute inflammatory injury by inhibiting the TLR4/MyD88/NF-κB signaling pathway in experimental traumatic brain injury. *J Neuroinflammation* 2014, 11:59.
53. Liu W, Wu YH, Zhang L, Xue B, Wang Y, Liu B, Liu XY, Zuo F, Yang XY, Chen FY, et al: MicroRNA-146a suppresses rheumatoid arthritis fibroblast-like synoviocytes proliferation and inflammatory responses by inhibiting the TLR4/NF-kB signaling. *Oncotarget* 2018, 9:23944-23959.

Figures

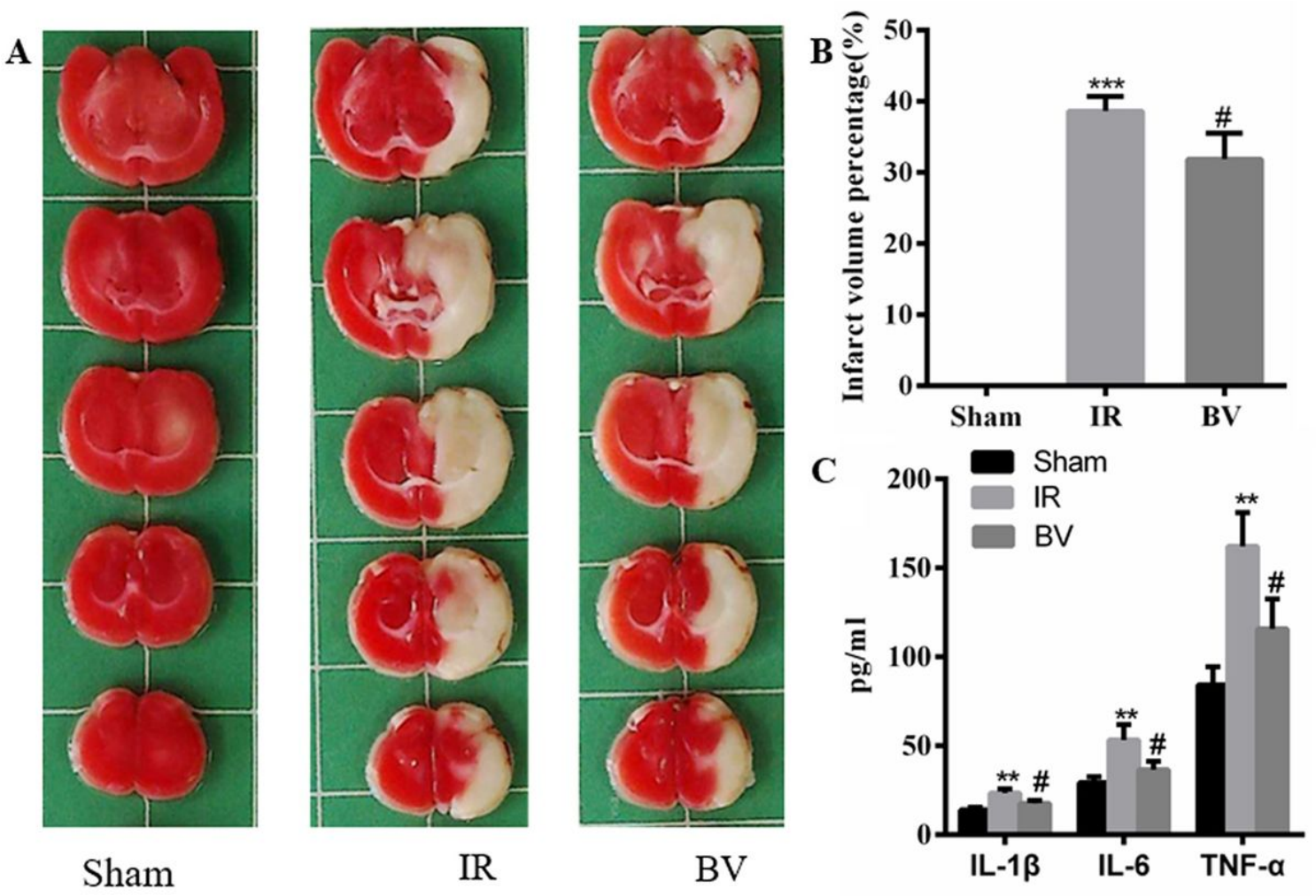

Figure 1

TTC staining and ELISA in the experimental groups. A Images of TTC staining in Sham, IR and BV groups. B The infarction volume % of cerebral hemisphere in the three groups. C Levels of serum IL-1β, IL-6 and TNF-α detected by ELISA. ***P<0.05, IR group vs Sham group, #P<0.05, BV group vs IR group.

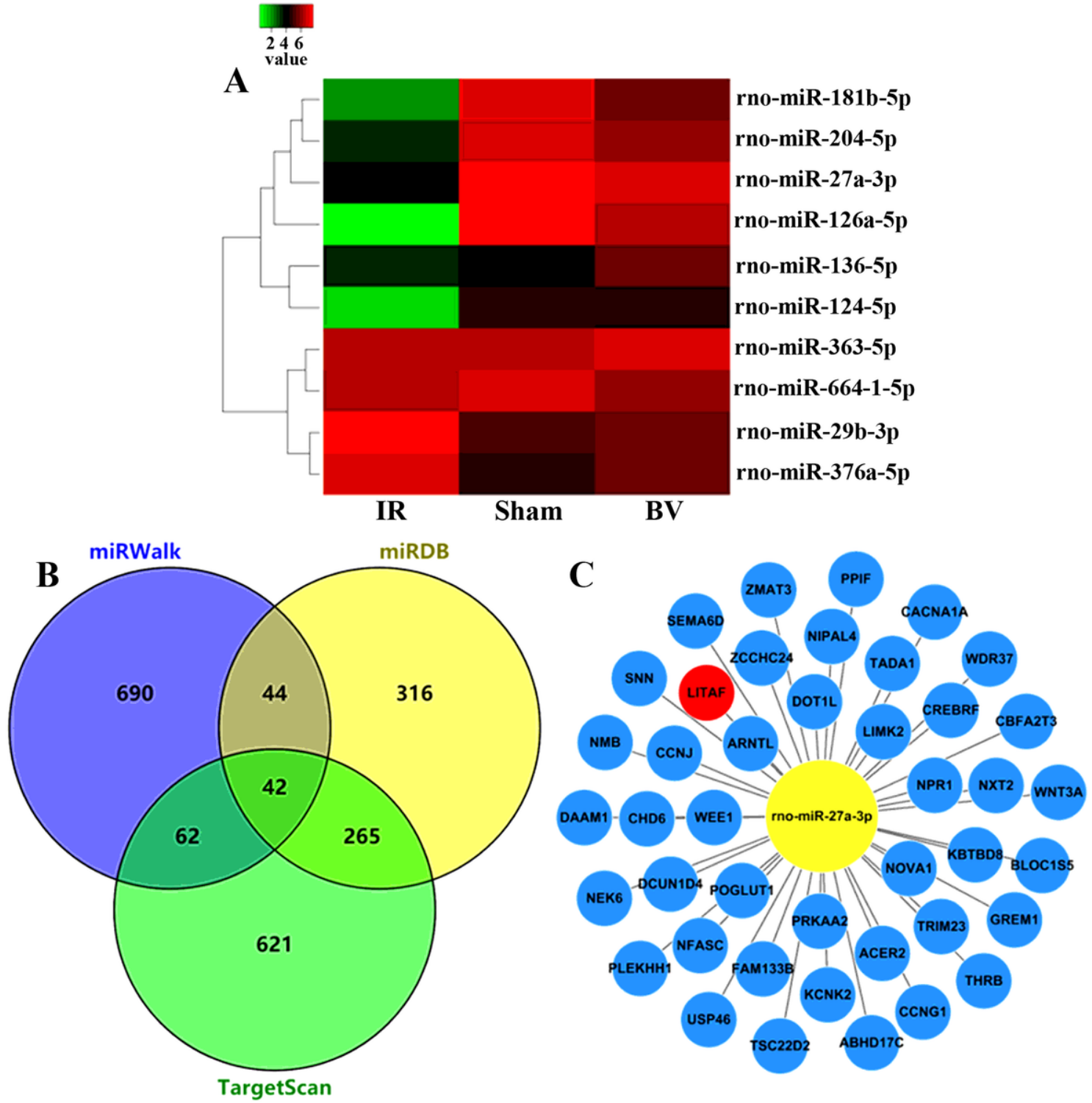

Figure 2

A Heatmap of the top 10 differentially expressed miRNAs in Sham, IR, and BV groups. The color code in the heat maps is linear with green as the lowest and red as the highest expression. B Venn diagram of targeted genes of miR-27a-3p got from miRWalk, miRDB and TargetScan databases. C Network between miR-27a-3p and its 42 targeted genes.

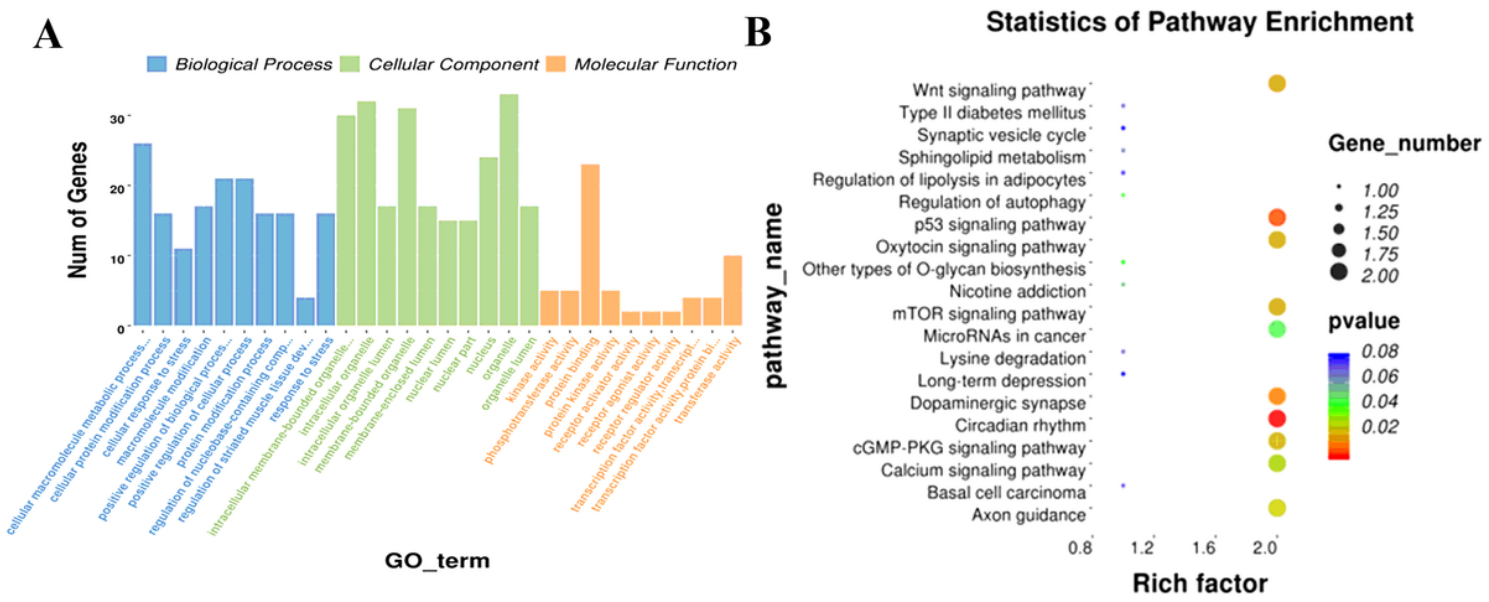

Figure 3

A GO analysis of 42 targeted genes of miR-27-3p. B KEGG pathway analysis of 42 targeted genes of miR-27-3p.

	Predicted consequential pairing target region(top) and miRNA(bottom)	Site type
Position 363-369 of LITAF3'UTR	5'...AUCUCGACCCCACUAACUGUGAU...	8mer
	|| || || ||	
Rno-miR-27a-3p	3' CGCCUUGAAUCGGUGACACUU	

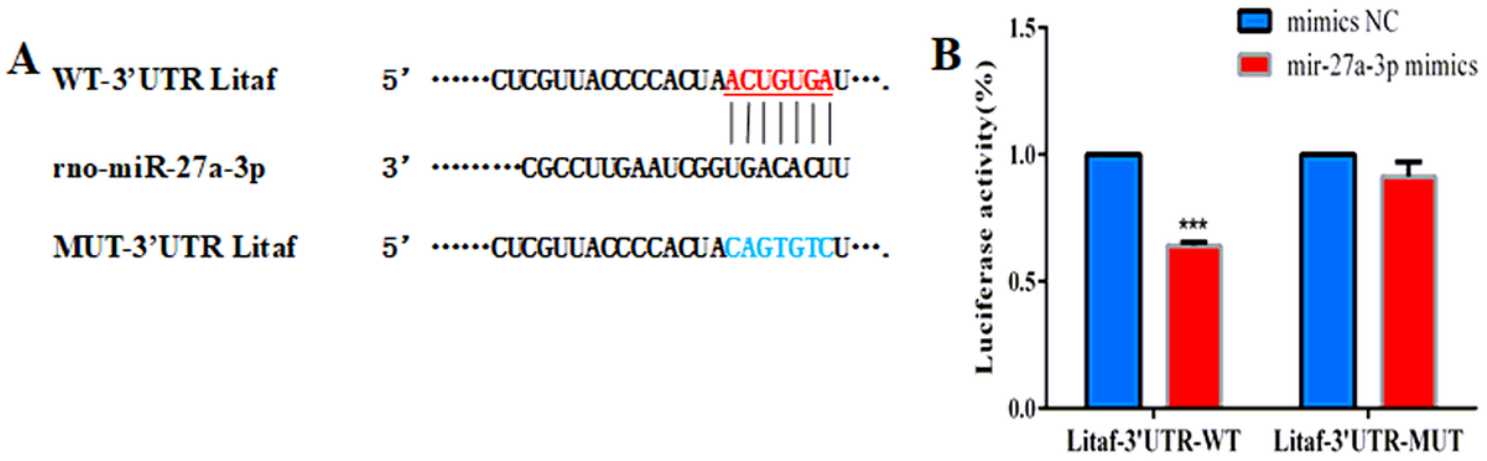

Figure 4

Identification of miR-27a-3p target site. UP: Schematic representation of the predicted interaction between miR-27a-3p and LITAF. A Pairing of miR-27a-3p to both 3'UTR of LITAF-WT and 3'UTR of LITAF-MUT. B Luciferase activity was measured in both wild type and mutant (MUT) LITAF 3'UTR and miR-27a-3p co-transfected cells. ***P<0.05 versus the control miR.

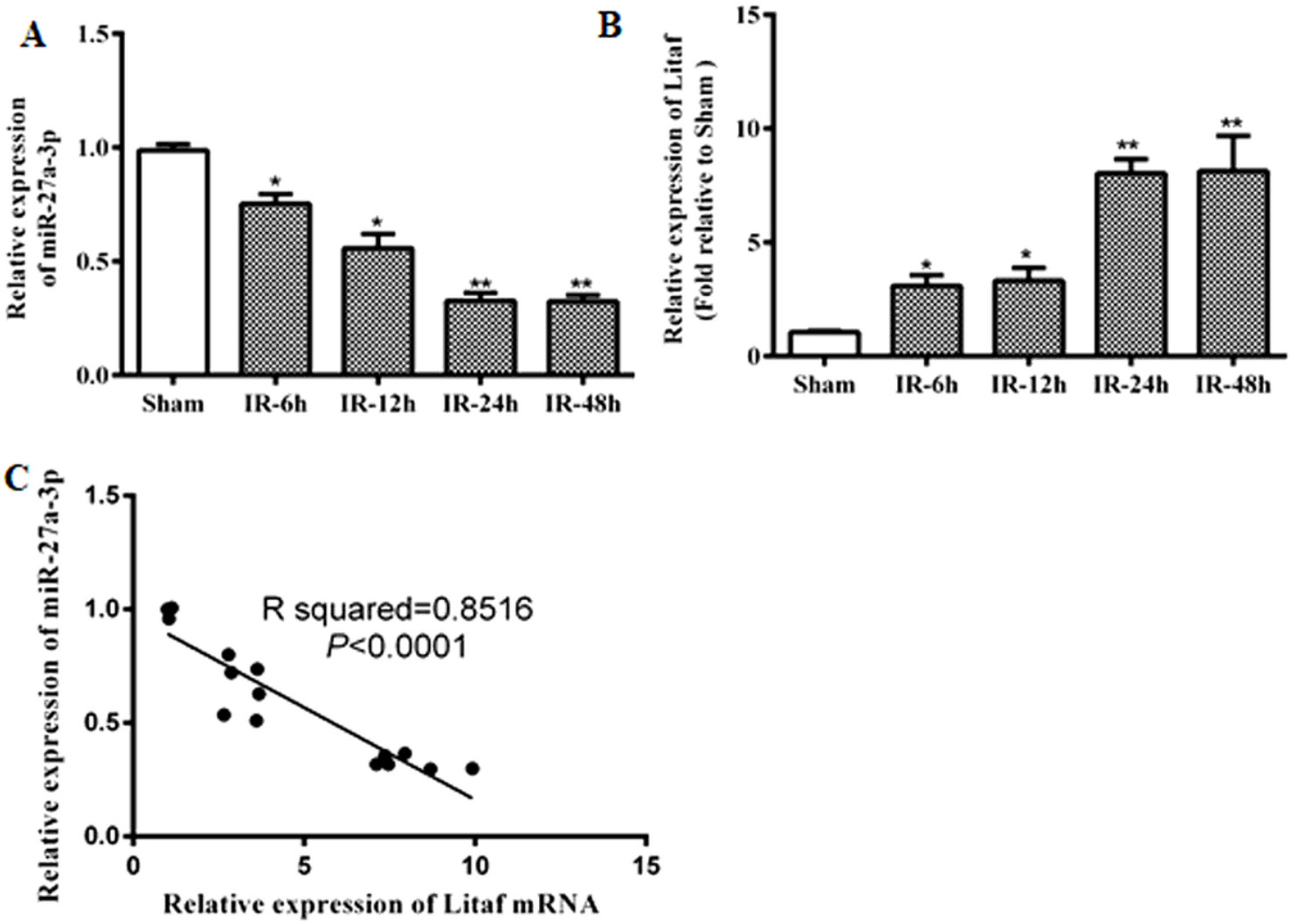

Figure 5

Time course of CIR-induced alterations in the miR-27a-3p and LITAF expression levels in rats with CIR injury. A Quantification of miR-27a-3p expression. B Quantification of LITAF expression. C Correlation analysis of miR-27a-3p and LITAF expression.

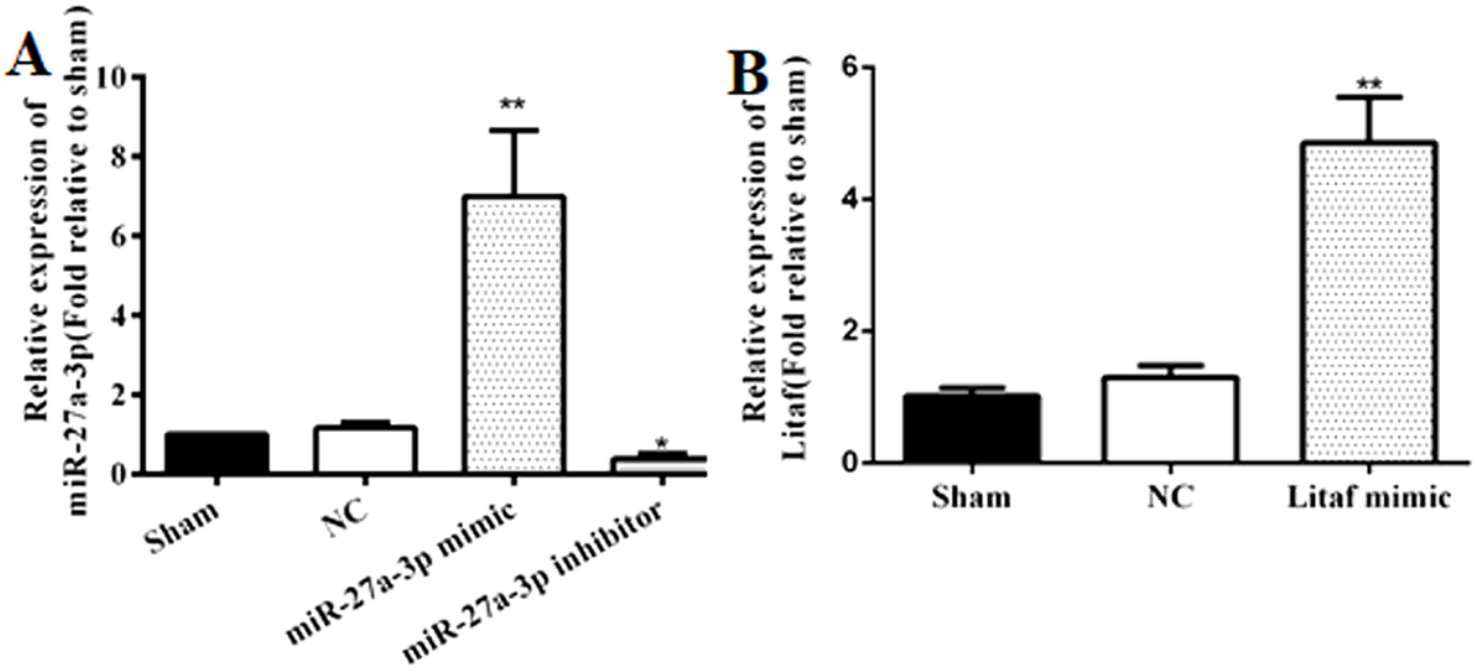

Figure 6

Time course of CIR-induced alterations in the miR-27a-3p and LITAF expression levels in rats with CIR injury. A Quantification of miR-27a-3p expression. B Quantification of LITAF expression. C Correlation analysis of miR-27a-3p and LITAF expression.

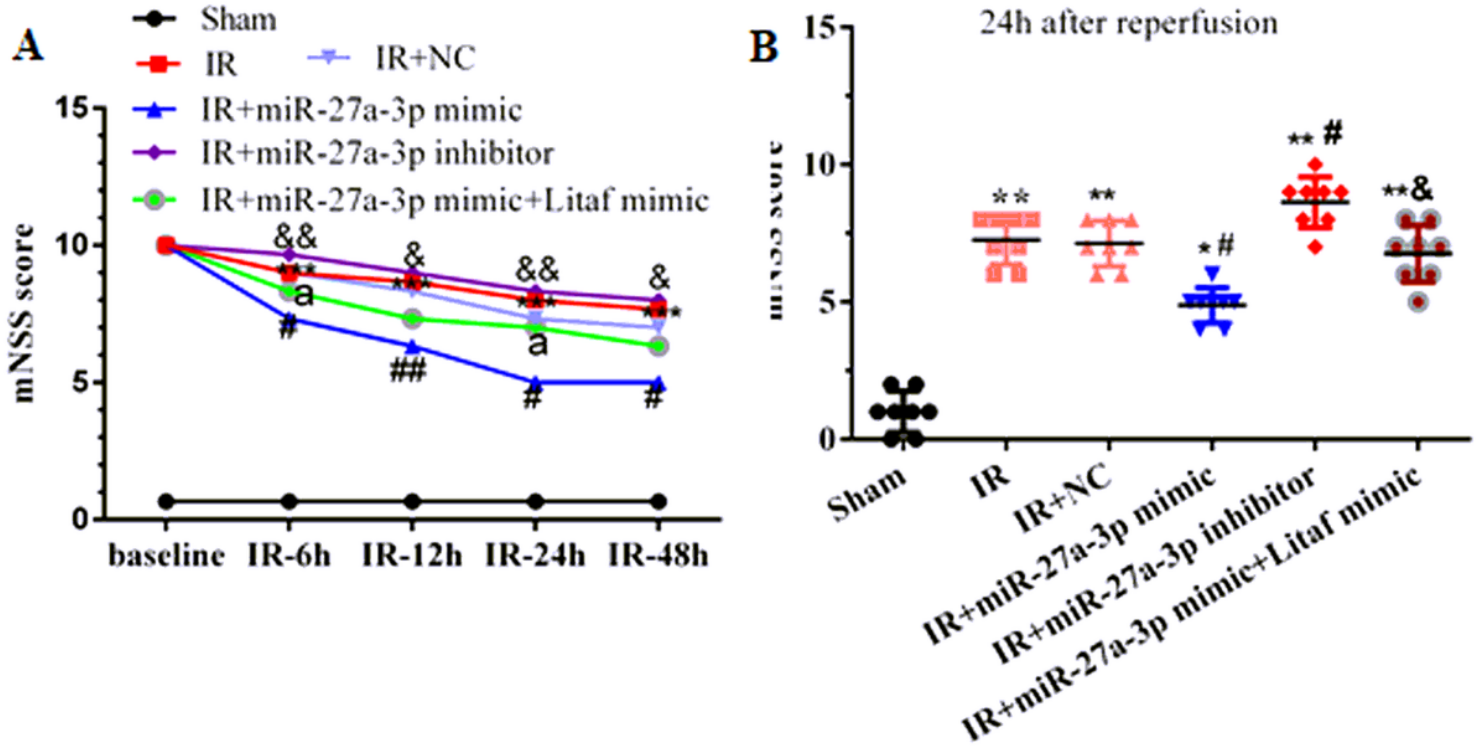

Figure 7

NSS test results in the six groups. A Modified NSS score in Sham, IR, IR+NC, IR+miR-27a-3p mimic, IR+miR-27a-3p inhibitor and IR+miR-27a-3p mimic + Litaf mimic groups at 6h, 12h, 24h and 28h after cerebral ischemia reperfusion. B Modified NSS score in Sham, IR, IR+miR-27a-3p mimic, IR+miR-27a-3p inhibitor and IR+miR-27a-3p mimic + Litaf mimic groups at 24 after cerebral ischemia reperfusion. Data are presented as mean ± standard deviation (n=3).

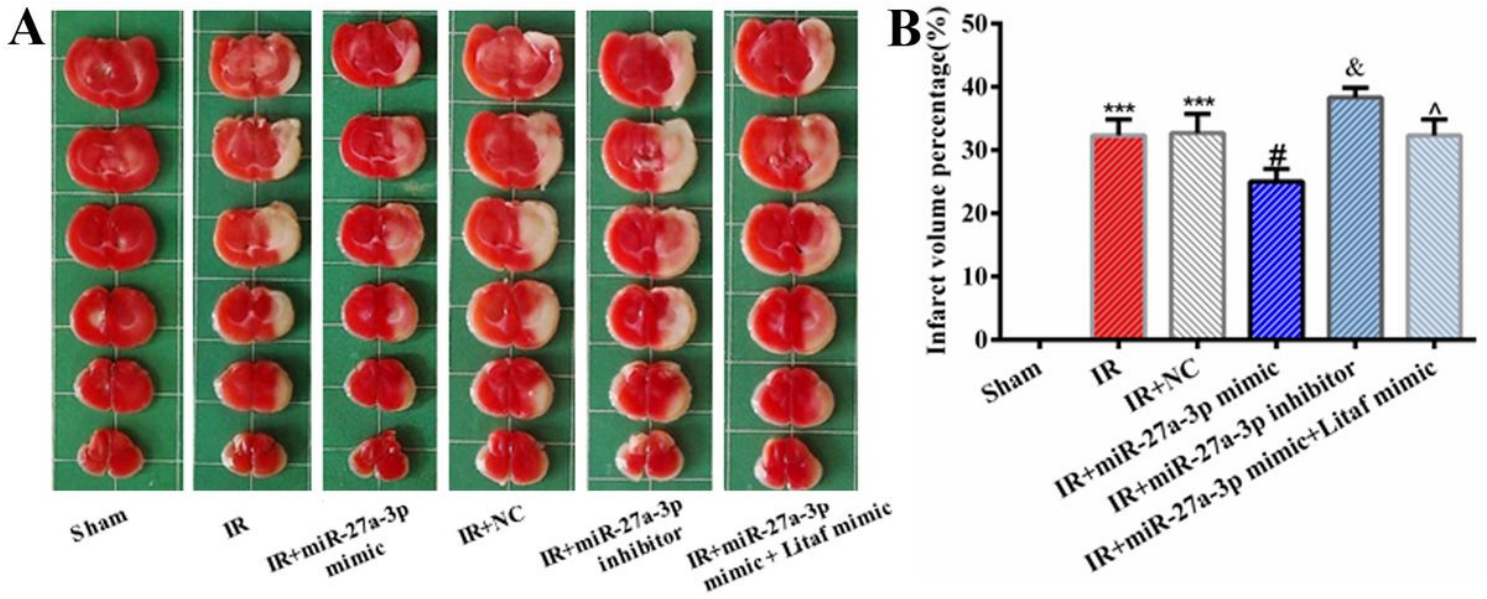

Figure 8

TTC staining in the experimental groups. A Images of TTC staining in Sham, IR and BV groups. B The infarct volume % of cerebral hemisphere in the three groups.

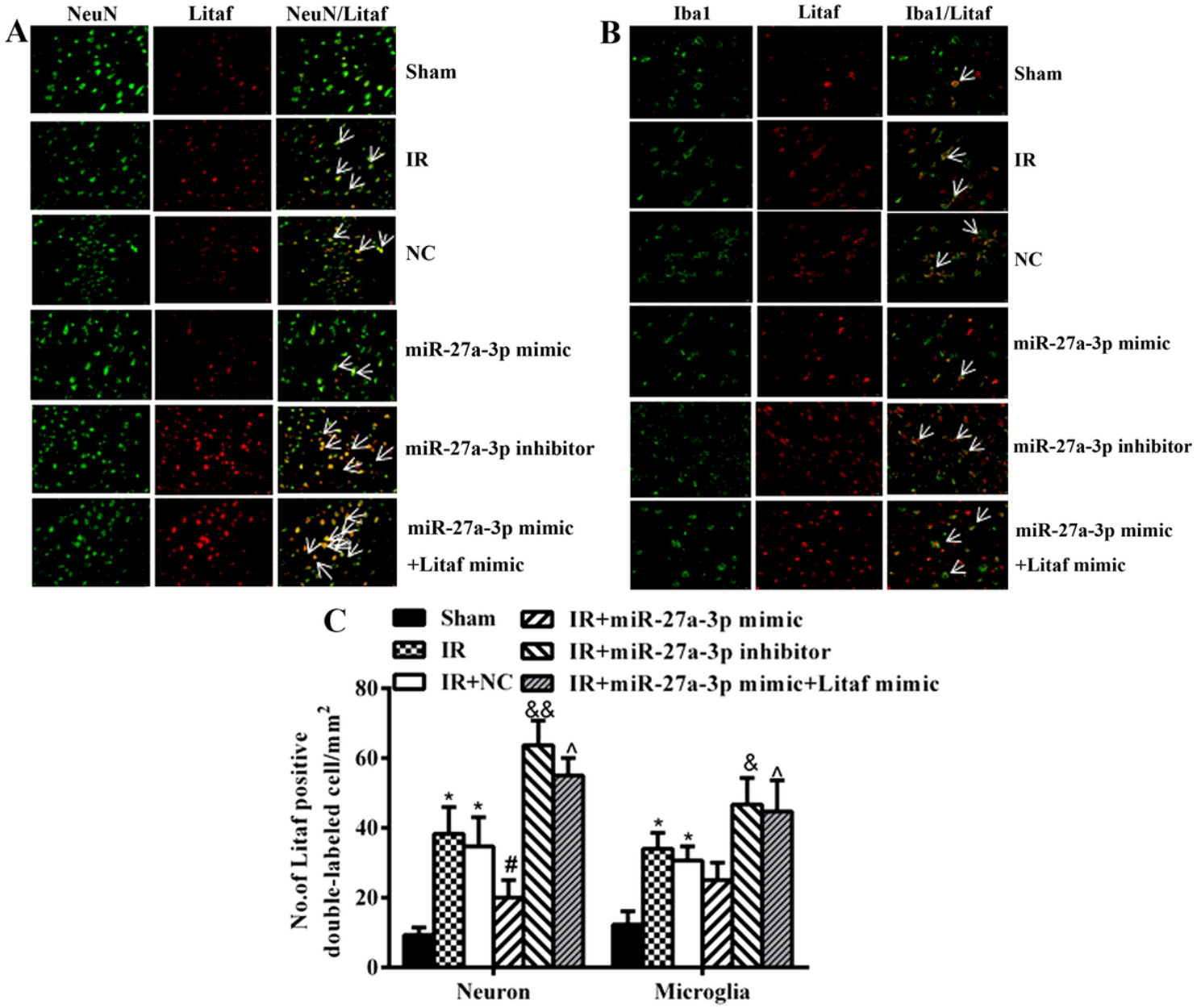

Figure 9

Effects of the miR-27a-3p mimic and inhibitor on LITAF expression in neuron and microglia of the cortex after CIR. A Representative fluorescence images showing the localization of the fluorescence signals for LITAF in neurons at 24h after CIR. Arrows indicate co-localization. Scale bars=20 μm. B Representative fluorescence images showing the localization of the fluorescence signals for LITAF in microglia at 24h after CIR. Arrows indicate co-localization. Scale bars=20 μm. C Quantification of LITAF-positive neurons and microglia in the cortex at 24h after CIR. Data are expressed as the mean ± SD.

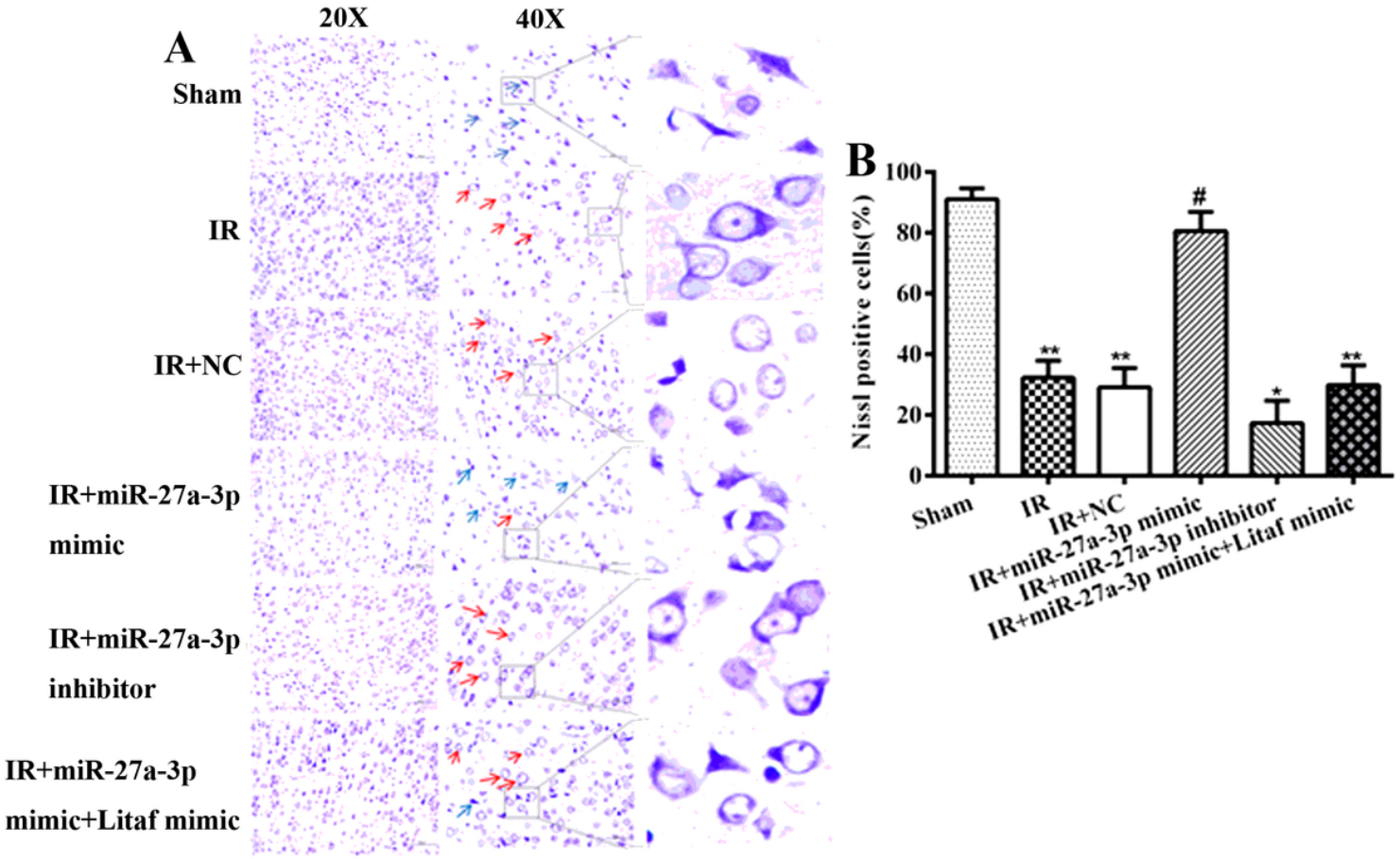

Figure 10

Drug treatment effect on the morphological alterations of Nissl staining in cortex after CIR injury. A: Representative images of Nissl staining in Sham, IR, IR+NC, IR+miR-27a-3p mimic, IR+miR-27a-3p inhibitor and IR+miR-27a-3p mimic + Litaf mimic groups. B Percentage of Nissl positive cells in different groups.

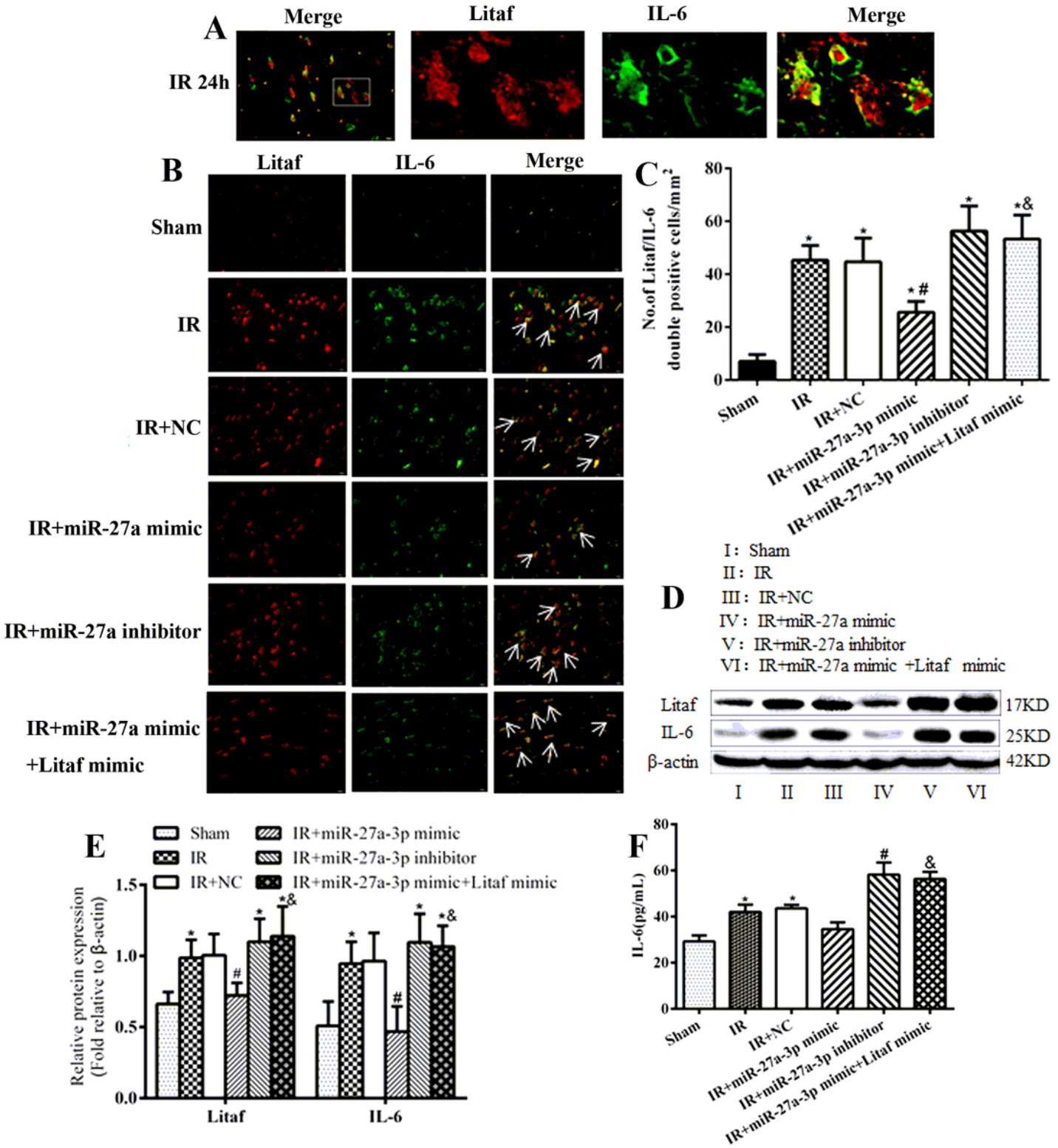

Figure 11

Effect of miR-27a-3p on the expression of Litaf/IL-6 at 24h after CIR. A Representative fluorescence images of the distribution of Litaf (red), IL-6 (green), nuclei (blue) and Merge (yellow). B Representative fluorescence images of the distribution of Litaf (red), IL-6 (green), nuclei (blue) and Merge (yellow) in Sham, IR, IR+NC, IR+miR-27a-3p mimic, IR+miR-27a-3p inhibitor and IR+miR-27a-3p mimic + Litaf mimic groups. D Representative western blots of Litaf and IL-6 in Sham, IR, IR+NC, IR+miR-27a-3p mimic,

IR+miR-27a-3p inhibitor and IR+miR-27a-3p mimic + Litaf mimic groups. β-actin was used as a loading control. E Quantification of the relative protein expression of Litaf and IL-6 at 24 h after CIR in Sham, IR, IR+NC, IR+miR-27a-3p mimic, IR+miR-27a-3p inhibitor and IR+miR-27a-3p mimic + Litaf mimic groups. F Serum IL-6 level in Sham, IR, IR+NC, IR+miR-27a-3p mimic, IR+miR-27a-3p inhibitor and IR+miR-27a-3p mimic + Litaf mimic groups.

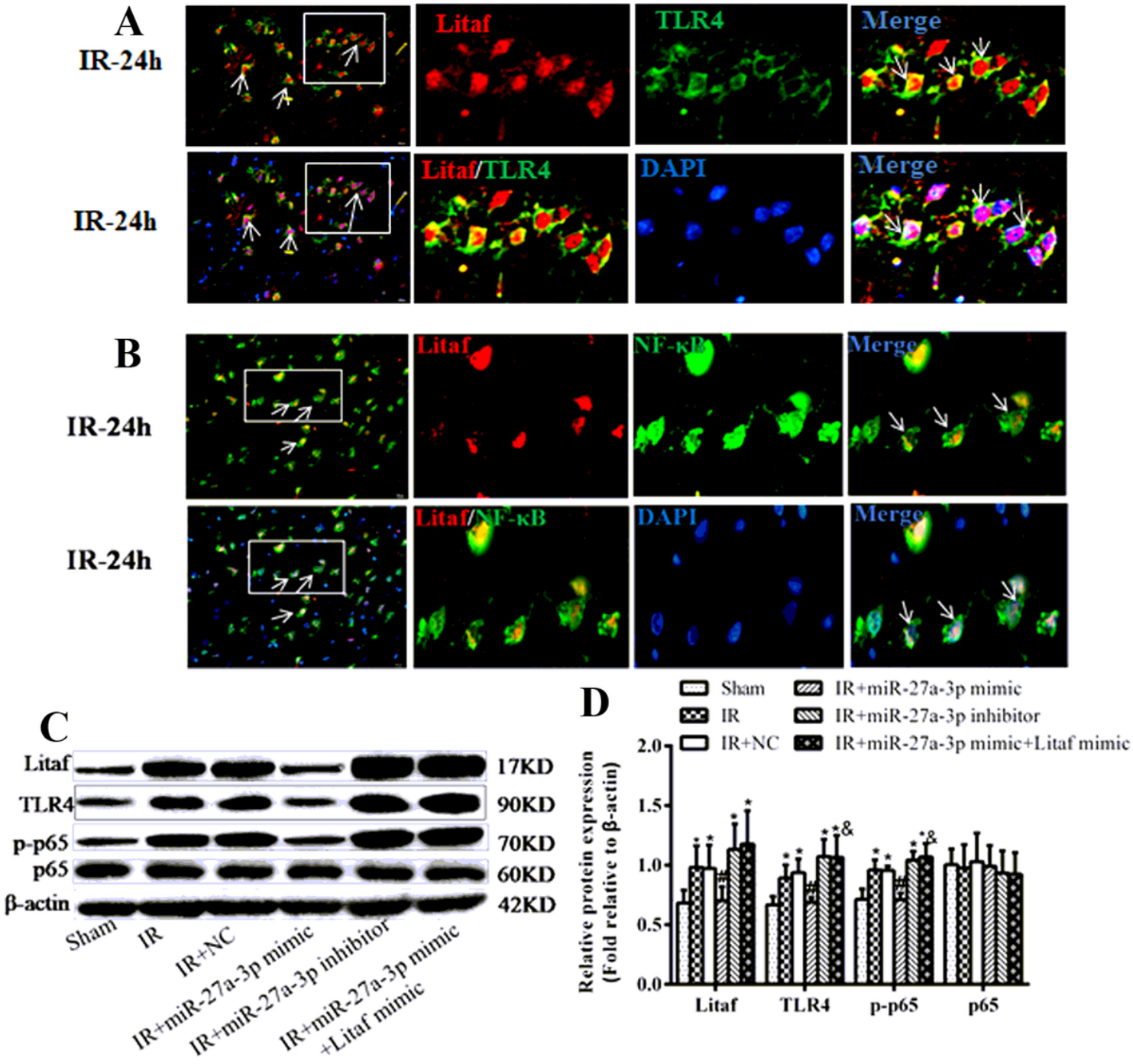

Figure 12

Effect of miR-27a-3p on the expression of TLR4/NF-κB at 24h after CIR. A Representative fluorescence images of the distribution of Litaf (red), TLR4 (green), nuclei (blue) and Merge (yellow). B Representative fluorescence images of the distribution of Litaf (red), NF-κB (green), nuclei (blue) and Merge (yellow). C

Representative western blots of Litaf, TLR4, p-p65 and p65 in Sham, IR, IR+NC, IR+miR-27a-3p mimic, IR+miR-27a-3p inhibitor and IR+miR-27a-3p mimic + Litaf mimic groups. β-actin was used as a loading control. D Quantification of the relative protein expression of Litaf, TLR4, p-p65 and p65 at 24 h after CIR in Sham, IR, IR+NC, IR+miR-27a-3p mimic, IR+miR-27a-3p inhibitor and IR+miR-27a-3p mimic + Litaf mimic groups.

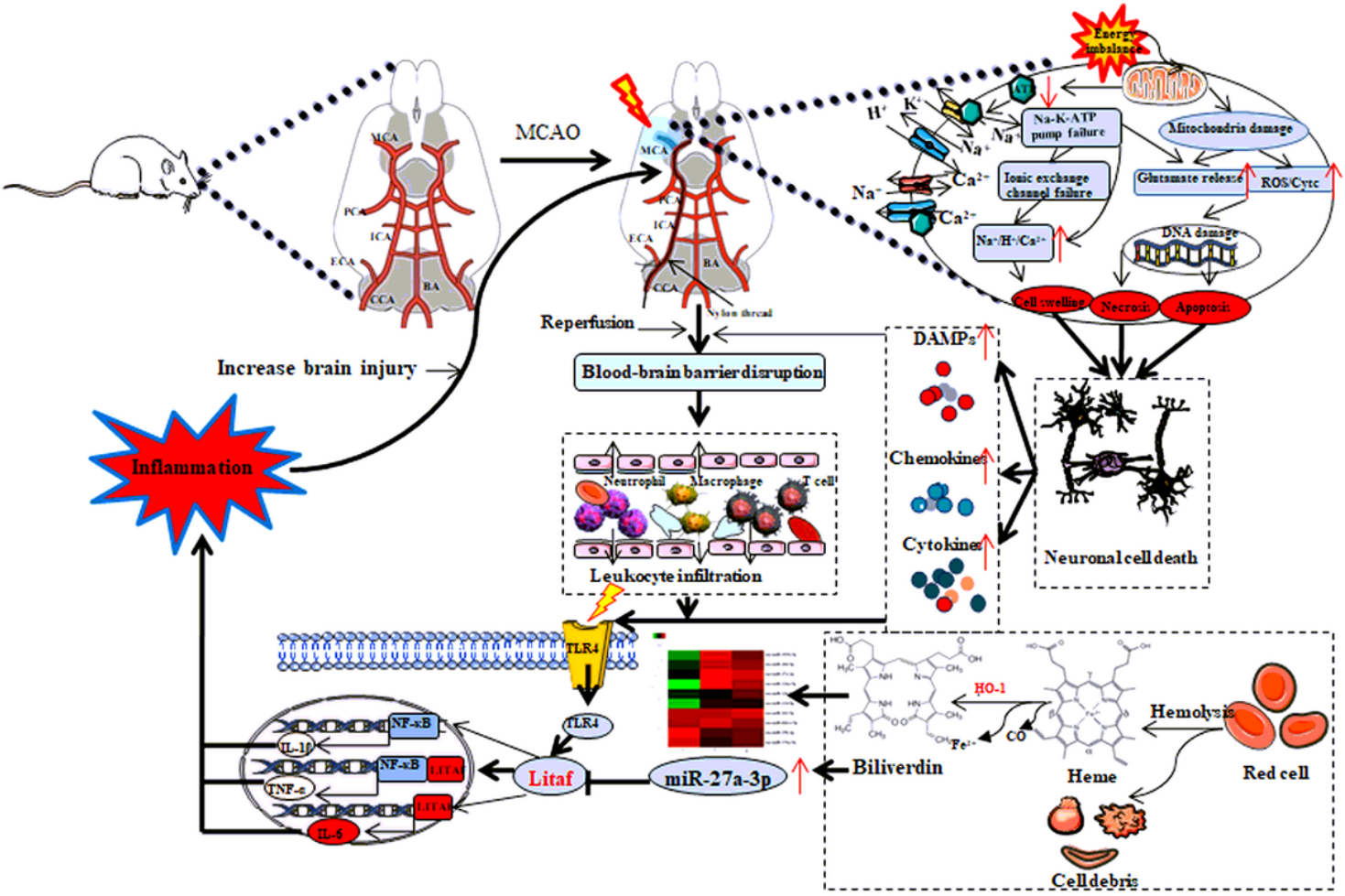

Figure 13

Experimental process showing miR-27-3p protect against CIR injury by relieving neuronal damage, cerebral infarct and neurologic deficit by inhibiting LITAF and the TLR4/NF-κB pathway